

**A HYBRID PIXEL-BASED CLASSIFICATION METHOD FOR BLOOD
VESSEL SEGMENTATION AND ANEURYSM DETECTION ON CTA**

**S. KOSTOPOULOS^a, D. GLOTSOS^a, G. C. KAGADIS^a, A. DASKALAKIS^a,
P. SPYRIDONOS^a, I. KALATZIS^c, M. KARAMESSINI^b, T. PETSAS^b,
D. CAVOURAS^c, AND G. NIKIFORIDIS^a**

*^aMedical Image Processing and Analysis Group, Laboratory of Medical Physics,
School of Medicine, University of Patras, 265 00 Rio, Greece*

^bDepartment of Radiology, University Hospital of Patras, 265 00 Rio, Greece

*^cMedical Image and Signal Processing Laboratory, Department of Medical
Instruments Technology, Technological Institute of Athens, 122 10 Athens, Greece*

Corresponding address:

Spiros Kostopoulos,
MIPA (Medical Image Processing and Analysis) Group
Laboratory of Medical Physics
School of Medicine
University of Patras
265 00 Rio, Greece
Tel: +30 2610 997745
Fax: +30 2610 996106
e-mail: skostopoulos@upatras.gr

Abstract

In the present study, a hybrid semi supervised pixel based classification algorithm is proposed for the automatic segmentation of intracranial aneurysms in Computed Tomography Angiography images. The algorithm was designed to discriminate image pixels as belonging to one of the two classes: blood vessel and brain parenchyma. Its accuracy in vessel and aneurysm detection was compared with two other reliable methods that have already been applied in vessel segmentation applications: a/ an advanced and novel thresholding technique, namely the Frequency Histogram of Connected Elements (FHCE), and b/ the gradient vector flow snake. The comparison was performed by means of the segmentation matching factor that expressed how precise and reproducible was the vessel and aneurysm segmentation result of each method against the manual segmentation of an experienced radiologist, who was considered as the gold standard. Results showed a superior segmentation matching factor (SMF) for the Hybrid (SMF=88.4%) and Snake (SMF=87.2%) methods compared to the FHCE (SMF=68.9%). The major advantage of the proposed hybrid method is that it requires no a priori knowledge of the topology of the vessels and no operator intervention, in contrast to the other methods examined. The hybrid method was efficient enough for use in 3D blood vessel reconstruction.

Keywords: vessel segmentation; CTA; PNN; Snake; FHCE

1. Introduction

An aneurysm is an abnormal bulging outward of an artery. Brain aneurysms (also called intracranial aneurysms) are commonly located at the branching points of the major blood vessels at the base of the brain. Intracranial aneurysms are usually discovered after they rupture, causing subarachnoid hemorrhage (SAH), i.e. bleeding in the subarachnoid space [1, 2]. A recent review [3] indicates a prevalence in the general population of up to 6%.

SAH is a serious condition with high morbidity and mortality. At 75% of the cases, SAHs are due to ruptured intracranial aneurysms (IAs), which usually originate from the major blood vessels of the cerebral arterial circle (circle of Willis) or from their branching arteries [4].

Detection of IAs has been traditionally performed using standard Digital Subtraction Angiography (DSA) [5]. Computed Tomography Angiography (CTA) is a new non-invasive imaging modality that has recently started to be recognized as a rapid and accurate alternative to the standard DSA technique for brain aneurysms visualization [6-9].

Brain aneurysm detection is of crucial importance, since it enables the quantification of a variety of crucial parameters (i.e. the width of the neck of the aneurysm, its orientation, and its relation to the parent vessel), that significantly affect treatment planning and surgical intervention [2, 6]. Thus, accurate detection and segmentation of brain blood vessels in CT angiograms is of major importance to the radiologists.

Although numerous studies and reviews have been devoted to the demanding task of vessel segmentation [10-14], from the technical aspect, there is no general technique that may be effectively applied to all modalities [12]. Regarding CTA, most previous studies have used inbuilt CT-software to segment aneurysms [5, 8], others have employed commercial software to outline aneurysms [6, 9], and few have experimented with own developed software for segmentation [10, 13, 14]. However, most segmentation techniques require a priori knowledge and/or operator intervention. Snakes (Active Contours) have been shown to be among the most promising techniques [10, 14, 15]. Another promising segmentation method is the pixel-based classification, employing supervised or unsupervised classifiers [16-18],

that require no a priori information and, to our knowledge, have found no application in vessel segmentation.

In the present study, a hybrid semi supervised pixel-based segmentation algorithm for the segmentation of aneurysms on CTA is proposed and it is compared against two other novel and reliable techniques that have been previously tested in vessel segmentation applications: an advanced thresholding technique, using connected elements, that has been employed in vessel segmentation on DSA images, and an advanced snake method [19], that has been previously used in aneurysm segmentation on CTA images.

2. Material and Methods

Eleven cases of patients with intracranial aneurysm were examined. From each case, a DICOM (Digital Imaging and Communications in Medicine) dataset of CTA brain images (Siemens Somaton Plus 4, Siemens, AG, Erlangen, Germany) were acquired from the Department of Radiology of the University Hospital of Patras, Greece. Datasets comprised 924 CTA images in total. CTA data slices were interpreted, using a typical window width (150 HU) and window center (100 HU), by an expert radiologist (T.P). As the basic interest was focused onto the major brain blood vessels, from where the aneurysm originated, a square (256x256) was cropped from the CT images resulting in images with primarily blood vessels and brain parenchyma.

An experienced radiologist (M.K) delineated manually the aneurysm (and its attached vessel) at each CT image slice twice, within a week's time interval, to investigate intra-observer delineation error. Figure 1 concerns one case with the aneurysm outlined by the radiologist in 12 out of 24 CT slices that the aneurysm extended.

2.1. Hybrid semi supervised pixel based classification method

Hybrid Classifier Design

A pixel-based segmentation algorithm, employing the probabilistic neural network (PNN) classifier [20], was designed to discriminate image pixels as belonging to one of two classes: blood vessel and brain parenchyma. The design of the classifier requires that an adequate number of class-patterns (combination of textural features, extracted from 5x5 regions of interest surrounding each pixel) have to be selected from the images. One third of the images of all cases was randomly chosen and used to design the hybrid classifier (training set) and the remaining images were employed to evaluate the classifier's performance (testing set). From each image of the design set, class-patterns were selected from the blood vessel and brain parenchyma regions. In most pixel-based segmentation algorithms [16, 17], selection of image-samples, to form class-patterns, has been performed manually. Such image-sample collection procedures, however, introduce users' subjectivity and suffer from a limitation concerning the maximum number of samples that the physician is prepared to collect. To alleviate this, the selection of image-samples regions was performed automatically

using an unsupervised (requires no training) *k-means* clustering methodology, which, combined with the supervised (requires training) pixel-based classification technique, it formulated the proposed hybrid algorithm (see Figure 2).

The k-means [21] was designed to take as input patterns the image pixel intensities, while the goal was to divide the patterns into 2 clusters; one containing the vessels' pixels and the other the parenchyma's pixels.

The algorithm divided the image pixels according the following procedure:

1. Two pixels were (randomly) selected as the initial cluster's centroids.
2. The rest of the image pixels were distributed to the two clusters, following the minimum Euclidean distance rule from its centroid.
3. New class centroids were calculated.
4. Steps 2 and 3 were repeated until both cluster-centroids stabilized.

Finally the last cluster's centers were used to define the median (discriminant of the clusters) that was the threshold value applied to each image.

Following this clustering process, the coordinates of image-samples from the vessel and parenchyma regions (see Figure 3) of the training set were used to optimally design the PNN classifier. From each one of the image-samples, 38 textural features were extracted, to form the class-patterns, by evaluating first and second order statistics: four features were computed from the image-sample histogram [22], 24 from the co-occurrence matrix [23, 24], which encodes the frequency of appearance of the same gray-tone pixel pairs of a particular inter-pixel distance inside each ROI (see appendix B), and 10 from the run-length matrix [25], which describes the frequency of appearance of a set of consecutive pixels having the same gray value.

The PNN classifier training aimed to locate the best feature combination that gave the highest classification accuracy with the least number of features. Classifier training involved the following steps:

1/Feature reduction. This was accomplished by reducing the number of possible features to 10, employing the students t-test, ranking the features in accordance with their class discriminatory power, and pick the first 10 features with the highest discriminatory power. This was a necessary step taken to reduce problem dimensionality and classifier's design computational time demands.

2/Best feature combination. The exhaustive search algorithm [26] (forming feature patterns ensembles in all possible combinations of 2, 3, 4, and 5 features) was used to design and, subsequently, to evaluate the accuracy of the PNN classifier, in the

attempt to locate the best feature combination, that provided the highest classification accuracy with the least number of features. Thus, for a particular feature combination, the PNN classifier was designed by all the feature patterns of the training set and it was used to classify all the feature-patterns (and eventually the corresponding pixels) of the testing set. The accuracy of classification was tested against the physician's accuracy (used here as gold standard) in manually outlining the vessels in each image and, thus, assigning image pixels as belonging to either the blood vessel or parenchyma class.

The final hybrid classifier comprised the k-means clustering algorithm that drives the PNN classifier, which was designed by the optimum of features, as described in steps 1 and 2 above. The hybrid classifier design is quite lengthy and computational demanding process. For example, it took 841 seconds for the exhaustive search only to test all possible 3-feature combinations. However, it needs to be performed once, since it is only employed in the optimal classifier design stage. Hybrid classifier design is not part of the classifier operation, which is a low time consuming process, as explained in the next section.

Hybrid Classifier Operation

Segmentation was performed by employing the optimally designed hybrid classifier on all images of the test set. In each image, the k-means classifier automatically separated image pixels into two classes, blood vessels and brain parenchyma, and the PNN worked on those pixels contained only within each vessel and its vicinity in the following manner. Each vessel region was automatically bounded by a box, the box's size was increased by 50% to incorporate missed boundary pixels by the k-means, and the PNN classifier scanned each pixel of the enlarged vessel-box using a 5x5 pixel window with one pixel step. At each step, the best feature combination was calculated and was used as input to the PNN classifier (see appendix A) to characterize the central pixel as belonging to one of the two classes: blood vessel and brain parenchyma. The result of the segmentation procedure was a binary image, with white pixels signifying the aneurysm-vessel class and black pixels the brain parenchyma class. Figure 2 shows a general overview of the hybrid method.

The proposed method in the present study was compared with other state-of-art segmentation methods, the Frequency histogram of connected elements (FHCE) [11] and the Active Contours (Snake) [19] (see appendix I).

2.2 Evaluation

The vessel segmentation accuracy for each method was tested using the *segmentation matching factor* (SMF) defined as the fraction of the intersection of A and B to the union of them [27].

$$SMF = A \cap B / A \cup B \quad (1)$$

where A is the area manually segmented by the Radiologist and B is the area segmented by each method (area is defined as the number of pixels included within the object's outline). Therefore, a factor nearer to unit indicates a segmented image closer to the expert's one. Moreover, the Coefficient of Variation ($CV\%$) was calculated for each method, that expresses the statistical representation of the precision of a method.

All methods were examined in terms of processing time, on a typical desktop PC (Pentium 4 @ 3GHz.with 512MB RAM). Regarding the proposed hybrid classifier, results indicated that the segmentation time per image ranged between 0.8 and 6 seconds, depending on the number of ROIs, containing vessels, in the image. Regarding the snake operation in consecutive data slices, automatic outlining of a vessel in a slice ranged between 2-4 seconds (employing the GVF algorithm and, as snake initialization points, the boundary data from the previous slice). However, in 30% of the consecutive data slices, user's interaction was necessary for redefining initialization points and, some times, for changing the values of the snake parameters, to achieve acceptable vessel boundary delineation. This amounted to a time processing overhead of about 6 seconds per image. Concerning FHCE, the algorithm functioned automatically, requiring about 1.5-1.7 seconds of processing time per image.

3. Results

Figure 3 illustrates the output regions of the k-means algorithm for vessels and brain parenchyma. From these regions, features were calculated to represent the vessels and brain parenchyma class respectively.

The features *mean value* (derived from the ROI's histogram), *inverse difference moment*, and *difference entropy* (co-occurrence matrix features, see appendix B) comprised the best feature vector combination, that optimized the performance of the PNN, in classifying aneurysm-vessel from parenchyma class with an accuracy of 94.4%. Additionally, to simulate more realistic conditions, all images of three randomly chosen patients were used in the training of the PNN classifier, using the previously determined best feature set. The PNN was then employed on the images of the remaining 8 patients to distinguish aneurysm-vessels from parenchyma. Accuracy was slightly lower than previously (92.4% against 94.4%), which however was expected, since patients in the test-set did not participate in the design of the classifier. Having chosen the training set (3 patients) and the best features combination, hybrid classifier training required approximately 2 seconds.

The results of such pixel-based segmentation are depicted in Figure 4. The light grey areas correspond to correctly segmented pixels, whereas the dark grey and white regions to erroneously segmented pixels, with respect to the manual delineation by the experienced Radiologist.

The radiologist's intra-observer reliability, in delineating manually the same vessels in a week's time interval, was examined revealing no significant difference between assessments ($p > 0.05$). The reproducibility, consistency, and accuracy of each segmentation method are summarized in the box plot of the SMFs in Figure 5.

Table 1 shows the SMF and the SMF's Coefficient of Variation ($CV\%$) for the *FHCE*, *Snake*, and *Hybrid* algorithms as well as for the intra-observer assessment of the Radiologist's delineation.

An isosurface rendering technique [28] was used for the three-dimensional volume reconstruction of segmented vessels (see Figure 6).

4. Discussion

In the present study, a hybrid semi supervised pixel based classification method was introduced for segmenting brain blood vessels and, thus, possible attached aneurysms. This hybrid algorithm comprised an unsupervised clustering algorithm (k-means) that led a supervised pixel-based segmentation algorithm, without any a priori knowledge of the shape and topology of the aneurysm to be segmented.

The proposed hybrid segmentation method was tested against two state-of-art segmentation algorithms, that have been previously implemented in vessel segmentation applications (snake and FHCE) [11, 12]. Results showed that the hybrid algorithm matched more closely ($SMF=88.4\pm 1.9\%$) the vessels outlines produced by the manual delineation of the experienced radiologist. The snake ($SMF=87.21\pm 2.2\%$) algorithm gave slightly inferior results, whereas the FHCE ($SMF=68.9\pm 2.4\%$) significantly inferior results (Table 1).

To quantitatively assess the precision and reproducibility of each method, the Coefficient of Variation ($CV\%$) of the SMF was calculated for each method (see Table 1). The hybrid method gave the best results in terms of $CV\%$, since it exhibited the smallest variability in repeated segmentations. This variability is graphically illustrated in the form of a box plot in Figure 5, where it is clear that the hybrid method gave the least variable results, compared to the FHCE and snake algorithms. The box plot provides a comprehensive visual view of the behaviour of each method in repeated segmentations. The location of the box plot corresponds to the accuracy of each segmentation method. The size of the box plot is an indication of reproducibility. The median value can be used to assess consistency. Under this perspective, the FHCE box plot gave the poorest accuracy and reproducibility with highly inconsistent results. On the other hand, the hybrid and snake gave the most consistent results, since their corresponding median values were located at the middle of the box (that is, the median values coincident with the respective mean values). The hybrid algorithm gave the most accurate and reproducible results and its box plot is closer to the radiologists, which is considered as the golden standard.

Although the FHCE has been shown promising results in vessel segmentation in DSA images [11], its performance on CTA images, used in the present study, was satisfactory with a SMF mean value of 68.9%. FHCE resulted into a ‘thinner segmentation’, underestimating the size of the vessels (see Figure 4). This might be

explained due to the fact that it is very difficult to define a specific threshold to optimize the FHCE algorithm's performance, since CTA images are composed of different anatomical structures (bone, parenchyma, vessels) with diverse pixel grey values, and with differences from slice to slice. On the other hand, in DSA images the background structures, such as bone and soft tissue shadows, are masked out during the acquisition process, thus, a threshold to separate vessels from background is easier to define.

Snakes constitute another family of methods that have been applied in vessel segmentation with promising results [12]. The snake, used in the present study, performed satisfactorily, as compared to the experts' manual segmentation, with an SMF mean value of 87.2%. The most significant problem with the snake algorithm was in cases of closely located vessels, where the image information was ambiguous. In such cases, the snake slightly expanded into parenchyma areas, resulting into small deviations from the vessel boundaries (see Figure 4). Another disadvantage of the snake was that it required manual initialization, that is, specification of the starting coordinates (curve points) by the radiologist. Even though the resulting snake boundaries for a particular vessel may be used as the initial curve points for delineation of the same vessel in the next slice, we have found that in 30 % of the cases, redefinition of initial points was unavoidable. Finally, setting parameters a and b that control the snake's tension and rigidity respectively required extensive experimentation.

The proposed hybrid method performed as well as the snake algorithm with an SMF mean value of 88.4%. However, it merits compared to the snake due to the following reasons: a) segmentation is performed automatically, b) no user interaction is required, and c) all vessels are simultaneously segmented.

Figure 6 shows the 3-dimensional geometric representation of segmented vessels, using by hybrid method, where the aneurysm is clearly delineated. This kind of 3-dimensional representation can be used to quantitatively measure a number of important parameters of vessels, such as the maximum diameter, the neck, the orientation, the number of bifurcations, the relation of smaller vessels to the parent vessels, and the presence of aneurysms. Additionally, it can be used to provide a comprehensive and accurate view of the vessels, thus, helping to achieve more accurate clinical diagnoses. As a general conclusion, the proposed hybrid segmentation might be useful as an efficient and practical tool for assisting

radiologists in 3-dimensional vessel visualization and aneurysms localization in brain CTA images.

Appendix A

The PNN algorithm

The Probabilistic Neural Network (PNN) classifier determines each class probability density function (PDF) by linearly combining the kernel PDF estimation for each training sample separately for a given class. Its discriminant function is given by [20]:

$$d_i(x) = \frac{1}{(2\pi)^{d/2} \sigma^d} \frac{1}{N} \sum_{k=1}^N \exp \left[-\frac{(x - x_{ik})^T (x - x_{ik})}{2\sigma^2} \right] \quad (\text{A.1})$$

where σ is the spread of the Gaussian activation function (smoothing parameter), N is the number of pattern vectors, d is the dimensionality of pattern vectors, x_{ik} is the k^{th} pattern vector of class i , and x is the unknown feature vector. The smoothing parameter σ was experimentally determined to be 0.2. The *PNN* classifies the input vector x to class j , if $d_j(x) > d_i(x)$.

The FHCE Method

The Frequency Histogram of Connected Elements (FHCE), proposed by Patricio and Maravall [11], is a novel approach used in digital image segmentation that takes into account the spatial properties of the image. FHCE not only embodies two concepts, the conventional image histogram (unidimensional) and the co-occurrence matrix (bidimensional), but it also empowers them by using the concepts of *connectivity level* and *morphological component* respectively.

FHCE is defined as [11]:

$$H(T) = \sum_{\forall (i,j) \in \{I\}} C_{i,j}(T), \quad 0 \leq T \leq I_{\max} - 1 \quad (\text{A.2})$$

where, I_{\max} is the maximum grayscale level of the image $I_{(i,j)}$, $C_{i,j}(T) \in [T - \varepsilon, T + \varepsilon]$ is the connected element, ε is the connectivity level and T is the gray level. The image was scanned and, at each pixel, a decision was made whether the morphological component constituted a connected element, in accordance with relation (A.2). The best morphological component, employed in the present application, was determined by trial and error to be the N4 neighborhood relation in 2D.

In that case, the central pixel's gray-level was used to form the frequency histogram of the connected components. Finally, a bimodal histogram was formed (one mode for each class), which was used to determine the threshold value that, in turn, was employed to transform the original gray level image into a binary segmented image, with white pixels corresponding to aneurysm-vessel class and black pixels to brain parenchyma class.

The Active Contours (Snake) Method

Snakes (Active Contours) have been successfully applied in the field of vessel segmentation [10, 12-14]. The operator must roughly determine the initial curve and the algorithm follows an iterative process until convergence to an optimum outline. Convergence is achieved by optimization of an energy functional that involves internal and external forces. Internal forces impose smoothness constraints on the curve, while external forces move the curve near the desired boundaries.

These models are characterized by limitations, not only on initializing the curve close to the boundaries to be detected, but, also, on expanding towards concave margins. In this study, a snake algorithm [19, 29] was used that took into account a field of external forces, called *gradient vector flow* (GVF), to overcome the above limitations. The snake model is given in (A.3):

$$E = \int_0^1 1/2 \cdot \left[a |x'(s)|^2 + b |x''(s)|^2 \right] + E_{ext}(x(s)) ds \quad (A.3)$$

where a and b are weight parameters that control the snake's tension and rigidity respectively, $x'(s)$ and $x''(s)$ are the first and second derivatives of $x(s)$, with respect to $s \in [0, 1]$, E_{ext} is the external energy function that leads the snake towards edges.

A snake that minimizes E must satisfy the Euler equation:

$$ax''(s) - bx'''(s) - \nabla E_{ext} = 0 \quad (A.4)$$

In order to find a solution for (A.4), snake parameter x treated as a function of time t as well as s . Therefore, the left hand side of (A.4) becomes:

$$x_i(s, t) = ax''(s, t) - bx'''(s, t) + F_{ext}$$

where

$$F_{ext} = -\nabla E_{ext}$$

The GVF field $v(x, y) = [u(x, y), v(x, y)]$ minimizes the energy functional

$$\mathcal{E} = \iint \mu(u_x^2 + u_y^2 + v_x^2 + v_y^2) + |\nabla f|^2 |v - \nabla f|^2 dx dy$$

where the parameter μ is a regularization parameter, governing the tradeoff between the first term and the second term in the integrant.

Parameters a , b and μ were experimentally determined as equal to 0.6 , 0.1 and 0.1 respectively.

Appendix B

Second order statistical features could be calculated from the co-occurrence matrix [23]:

$$p(i, j | d) = 1/4 \cdot \sum_{\Phi=0,45,90,135} p(i, j | d, \Phi)$$

Each $p(i, j | d, \Phi)$, is the probability of going from gray level i to gray level j , given that the intersample spacing is d and that the direction is given by angle Φ .

The best feature vector combination, used into the segmentation process of the hybrid algorithm, were

$$mean\ value = 1/N \cdot \sum_i \sum_j g(i, j)$$

$$Inverse\ Difference\ Moment = \sum_{i=0}^{N_g-1} \sum_{j=0}^{N_g-1} p(i, j) / (1 + (i - j)^2)$$

$$\text{Difference Entropy} = - \sum_{i=0}^{N_g-1} P_{x-y}(i) \log P_{x-y}(i)$$

where $g(i,j)$ is the pixel intensity in position (i,j) and N the total number of pixels, N_g is the number of gray levels in the image, $i,j=1 \dots N_g$, p is the co-occurrence matrix , and $P_{x-y}(k) = \sum_i \sum_{j, |i-j|=k} p(i, j)$.

Acknowledgements

We thank Greek State Scholarships Foundation (I.K.Y) for funding the above work.

References

- [1] Gasparotti R, Liserre R. Intracranial aneurysms. *Eur Radiol* 2005;15:441-7.
- [2] Schievink WI. Intracranial Aneurysms. *N Engl J Med* 1997;336:28-40.
- [3] Rinkel G, Djibuti M, Algra A, VAN GJ. Prevalence and risk of rupture of intracranial aneurysms: a systematic review. *Stroke* 1998;29:251-6.
- [4] Wardlaw JM, White PM. The detection and management of unruptured intracranial aneurysms. *Brain* 2000;123:205-21.
- [5] Tomandl BF, Kostner NC, Scempershofe M, Huk WJ, Strauss C, Anker L et al. CT Angiography of Intracranial Aneurysms: A Focus on Postprocessing. *Radiographics* 2004;24:637-55.
- [6] Karamessini MT, Kagadis GC, Petsas T, Karnabatidis D, Konstantinou D, Sakellaropoulos GC et al. CT angiography with three-dimensional techniques for the early diagnosis of intracranial aneurysms. Comparison with intra-arterial DSA and the surgical findings. *Eur J Radiol* 2004;49:212-23.
- [7] Chawla S. Advances in Multidetector Computed Tomography: Applications In Neuroradiology. *J Comput Assist Tomogr* 2004;28:S12-6.
- [8] Kangansiemi M, Makela T, Koskinen S, Porras M, Poussa K, Hernesniemi J. Detection Of Intracranial Aneurysms With Two-Dimensional And Three-Dimensional Multislice Helical Computed Tomographic Angiography. *Neurosurgery* 2004;54:336-41.
- [9] Villablanca JP, Jahan R, Hooshi P, Lim S, Duckwiler G, Patel A et al. Detection and characterization of very small cerebral aneurysms by using 2D and 3D helical CT angiography. *AJNR Am J Neuroradiol* 2002;23:1187-98.
- [10] Lorigo LM, Faugeras OD, Grimson WE, Keriven R, Kikinis R, Nabavi A et al. CURVES: curve evolution for vessel segmentation. *Med Image Anal* 2001;5:195-206.
- [11] Patricio MA, Maravall D. A Comparative Study of Contextual Segmentation Methods for Digital Angiogram Analysis. *Cybernetics and Systems: An International Journal* 2004;35:63-83.
- [12] Kirbas C, Quek F. A review of vessel extraction techniques and algorithms. *Acm Computing Surveys* 2004;36:81-121.
- [13] La Cruz A, Straka M, Köchl A, Šrámek M, Gröller E, Fleischmann D. "Non-linear Model Fitting to Parameterize Diseased Blood Vessels", in proceedings of IEEE Visualization Year, pp.393-400.

- [14] Subasic M, Loncaric S, Sorantin E. Model-based quantitative AAA image analysis using a priori knowledge. *Comput Methods Programs Biomed* 2005;80:103-14.
- [15] Siddiqi K, Vasilevskiy A. 3D Flux Maximizing Flows. *Lecture Notes In Copmuter Science* 2001;2134:636-50.
- [16] Spyridonos P, Ravazoula P, Cavouras D, Berberidis K, Nikiforidis G. Computer-based grading of haematoxylin-eosin stained tissue sections of urinary bladder carcinomas. *Med Inform Internet Med* 2001;26:179-90.
- [17] Spyridonos P, Cavouras D, Ravazoula P, Nikiforidis G. Neural network-based segmentation and classification system for automated grading of histologic sections of bladder carcinoma. *Anal Quant Cytol Histol* 2002;24:317-24.
- [18] Glotsos D, Spyridonos P, Cavouras D, Ravazoula P, Dadioti PA, Nikiforidis G. An image-analysis system based on support vector machines for automatic grade diagnosis of brain-tumour astrocytomas in clinical routine. *Med Inform Internet Med* 2005;30:179-93.
- [19] Xu C, Prince JL. Snakes, Shapes, and Gradient Vector Flow. *IEEE Transactions On Image Processing* 1998;7:359-69.
- [20] Specht DF. Probabilistic Neural Networks. *Neural Networks* 1990;3:109-18.
- [21] Jain AK, Dubes RC. *Algorithms for Clustering Data*. New Jersey: Prentice-Hall, 1988.
- [22] Theodoridis S, Koutroumbas K. *Pattern Recognition*. 2nd ed. San Diego: Academic Press, 1998.
- [23] Haralick RM, Shanmugam K, Dinstein IH. Textural Features for Image Classification. *IEEE Trans Sys Man Cyb* 1973;3:610-21.
- [24] Lohmann G. Analysis and synthesis of textures: A co-occurrence-based approach. *Computers & Graphics* 1995;19:29-36.
- [25] Galloway MM. Texture Analysis Using Gray-Level Run Lengths. *Computer Graphics and Image Processing* 1975;4:172-9.
- [26] Spyridonos P, Cavouras D, Ravazoula P, Nikiforidis G. A computer-based diagnostic and prognostic system for assessing urinary bladder tumour grade and predicting cancer recurrence. *Med Inform Internet Med* 2002;27:111-22.
- [27] Betal D, Roberts N, Whitehouse GH. Segmentation and numerical analysis of microcalcifications on mammograms using mathematical morphology. *Br J Radiol* 1997;70:903-17.

[28] Mathworks. Image Processing Toolbox. Available: <http://www.mathworks.com/access/helpdesk/help/techdoc/ref/ref.shtml> via the INTERNET. Accessed 2006 Mar 07.

[29] Xu C, Prince JL. Active Contours, Deformable Models, and Gradient Vector Flow. Available: <http://iacl.ece.jhu.edu/projects/gvf/> via the INTERNET. Accessed 2006 Mar 07.

Figure Captions:

Figure 1: Radiologist's delineation of aneurysm and attached vessel (Anterior Communicating Artery).

Figure 2: Overview of the hybrid method. k-means was used for automatically extracting the image-sample ROIs from region 1 (vessels) and region 2 (parenchyma tissue) and the PNN was trained, based on the extracted ROIs, to discriminate pixels belonging to vessel from pixels belonging to parenchyma.

Figure 3: The output of k-means that triggers the automatic feature extraction for the vessel (grayscale region) and parenchyma class (black region) respectively.

Figure 4: Segmentation results of all methods compared to the manual delineation of the experienced Radiologist. Light gray regions indicate correctly segmented pixels. White regions correspond to over segmented pixels: that is, erroneously segmented pixels outside the outlines marked by the Radiologist. Dark gray regions point to under segmented pixels: that is, erroneously unsegmented pixels located inside the outlines marked by the Radiologist.

Figure 5: Box plot of the SMFs between the Radiologist' manual segmentation and the second manual segmentation (RADIOLOGIST), the FHCE, the SNAKE and the HYBRID methods. The lower and upper lines express the data range, the lower and upper edges of the box indicate the 25th and 75th percentile. The line inside the box indicates the median value of the data.

Figure 6: 3D image of segmented vessel (Anterior Communicating Artery) and its attached aneurysm (black arrow). Viewpoint orientation at Azimuth:-68, Elevation: 42.

Tables:**Table 1:** Evaluation results of the examined segmentation methods expressed by the percentage SMF and the Coefficient of Variation (CV%) for each segmentation method.

Case	RADIOLOGIST	FHCE	SNAKE	HYBRID
1	<i>89.38</i>	<i>66.76</i>	<i>84.71</i>	<i>87.48</i>
2	<i>90.31</i>	<i>65.53</i>	<i>88.54</i>	<i>87.24</i>
3	<i>88.48</i>	<i>70.28</i>	<i>84.42</i>	<i>86.47</i>
4	<i>92.39</i>	<i>70.92</i>	<i>91.26</i>	<i>91.04</i>
5	<i>92.05</i>	<i>71.75</i>	<i>89.61</i>	<i>92.08</i>
6	<i>91.55</i>	<i>71.13</i>	<i>88.08</i>	<i>89.37</i>
7	<i>91.14</i>	<i>66.39</i>	<i>86.61</i>	<i>86.41</i>
8	<i>88.78</i>	<i>66.35</i>	<i>84.31</i>	<i>86.05</i>
9	<i>91.24</i>	<i>69.94</i>	<i>86.63</i>	<i>89.26</i>
10	<i>89.14</i>	<i>68.06</i>	<i>87.11</i>	<i>89.44</i>
11	<i>90.16</i>	<i>71.82</i>	<i>88.01</i>	<i>87.89</i>
Mean Value	<i>90.42</i>	<i>68.99</i>	<i>87.21</i>	<i>88.43</i>
Standard Deviation	<i>1.35</i>	<i>2.41</i>	<i>2.20</i>	<i>1.97</i>
CV (%)	<i>1.49</i>	<i>3.49</i>	<i>2.52</i>	<i>2.23</i>

Figure 1
[Click here to download high resolution image](#)

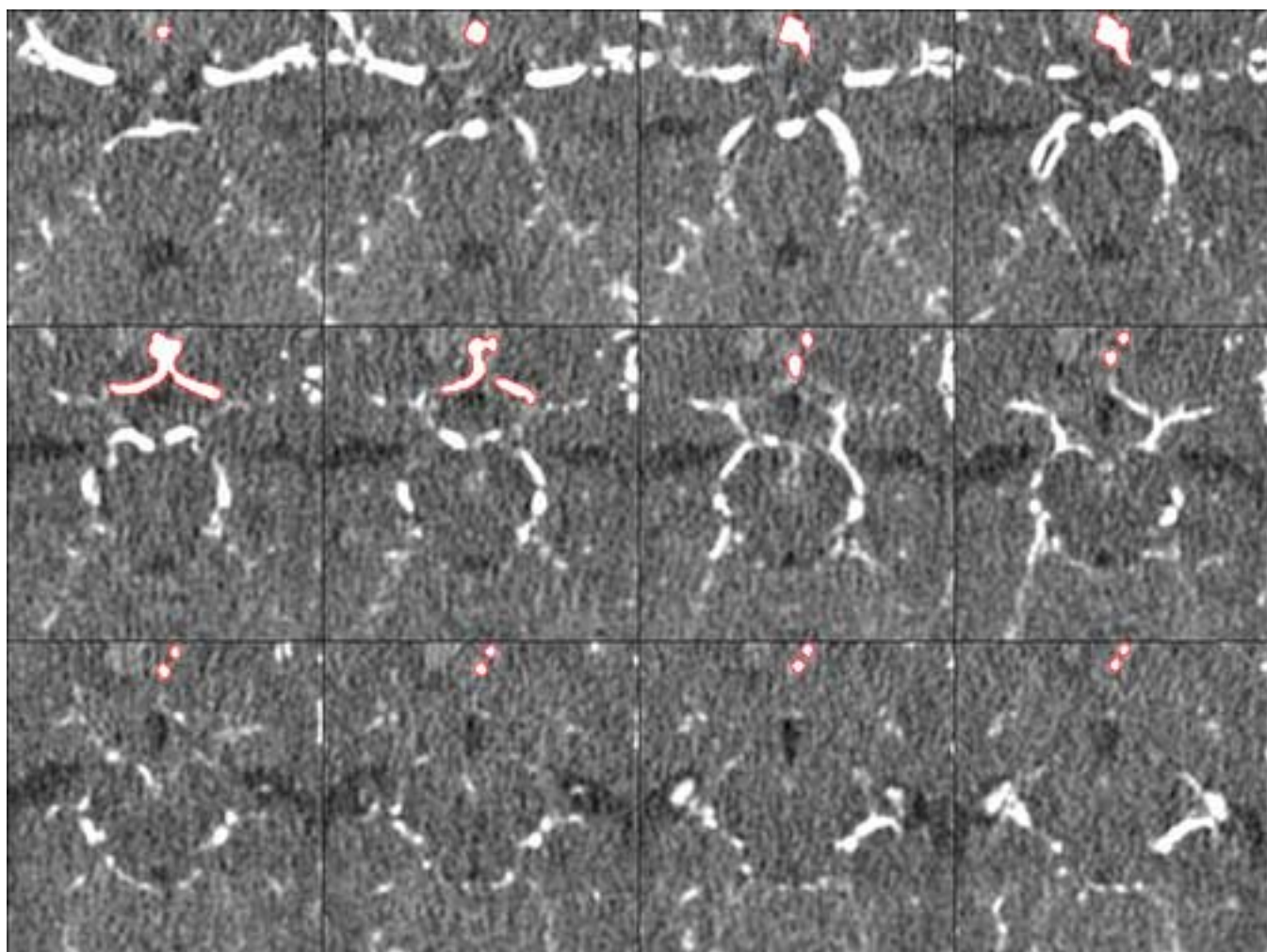


Figure 2

[Click here to download high resolution image](#)

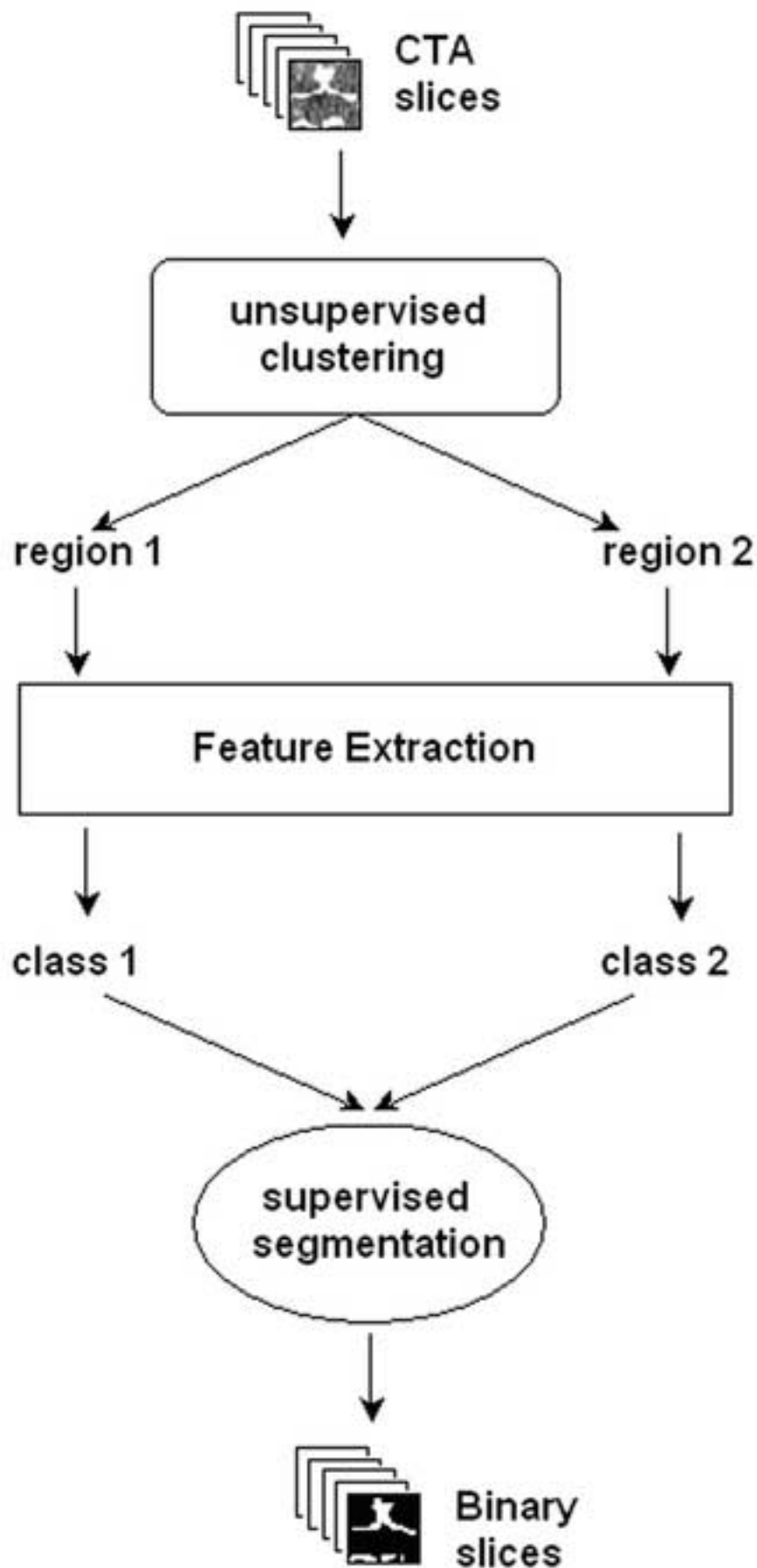


Figure 3
[Click here to download high resolution image](#)



Figure 4
[Click here to download high resolution image](#)

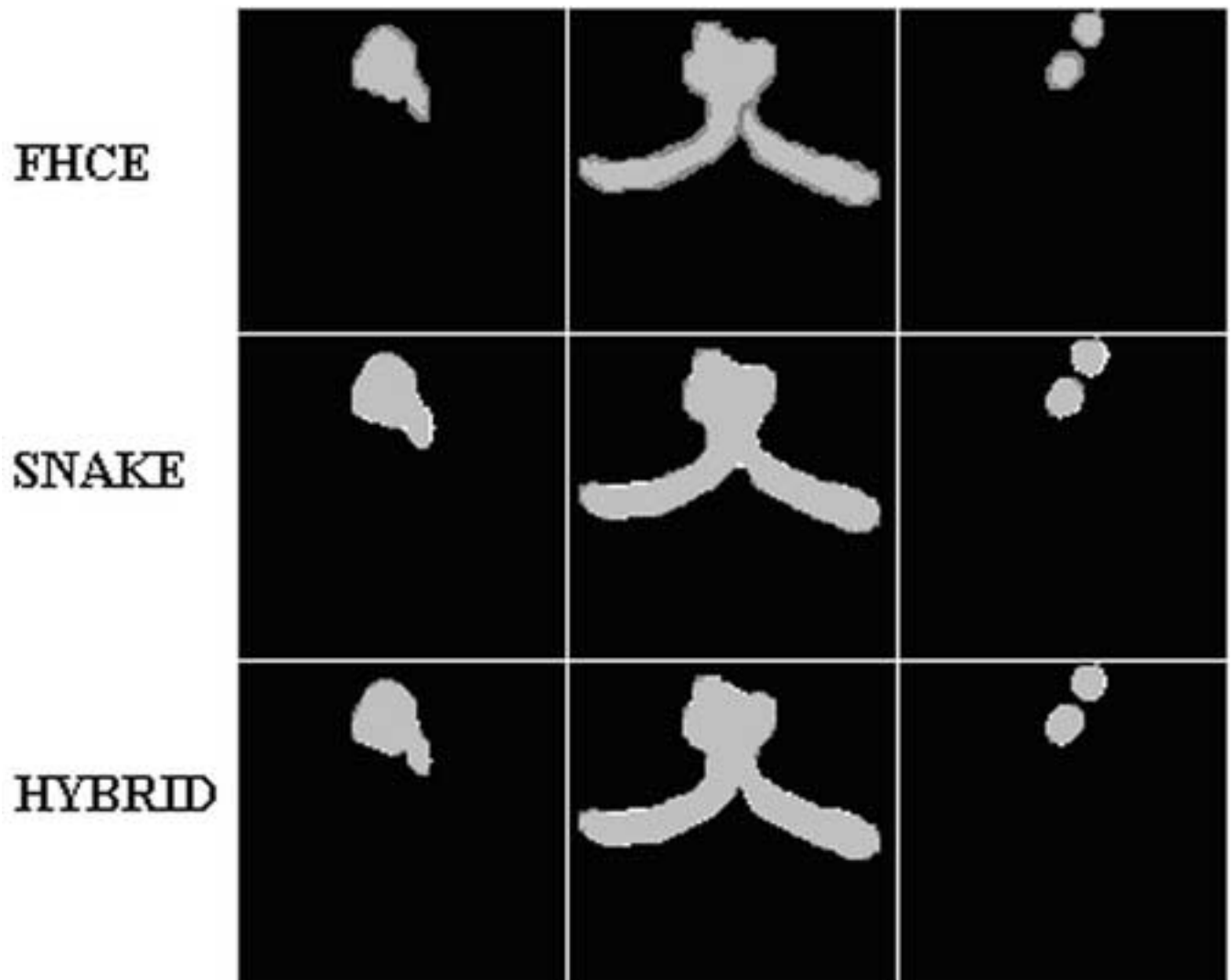


Figure 5
[Click here to download high resolution image](#)

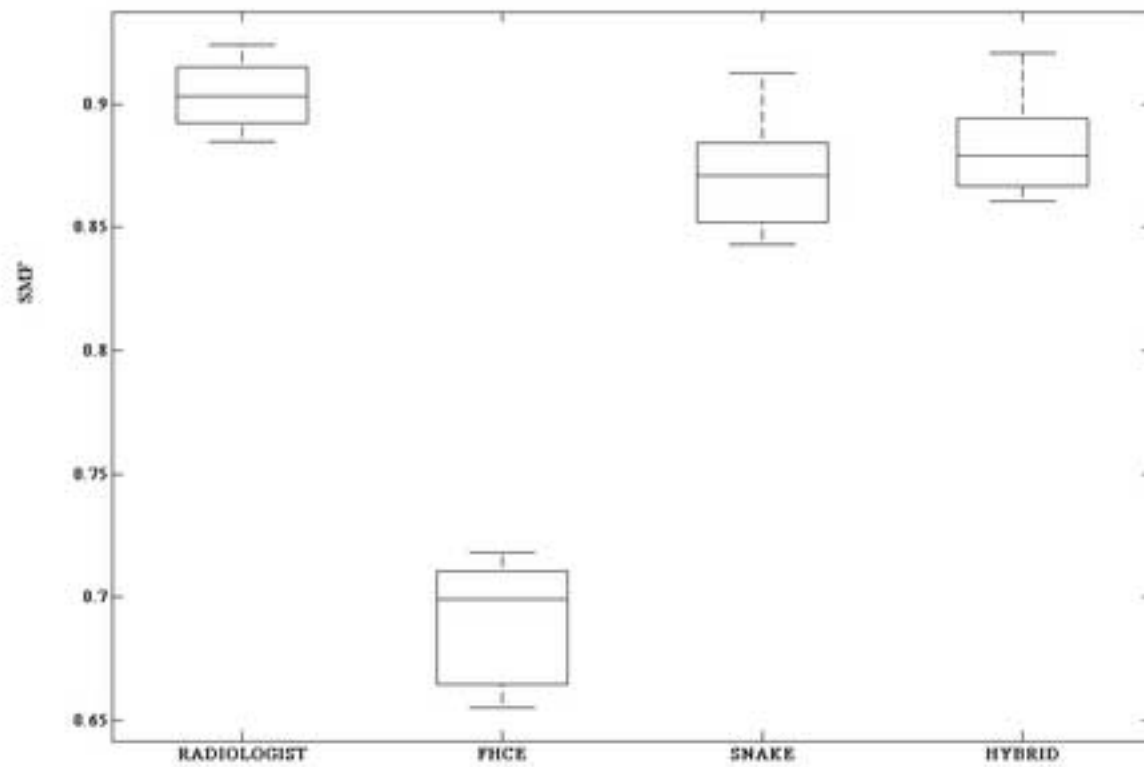


Figure 6
[Click here to download high resolution image](#)

